

Measurement of the branching fractions for $B^+ \rightarrow (c\bar{c})K^+ \rightarrow p\bar{p}K^+$ decays

Jae Keum Lee^{*†} and Stephen Lars Olsen

Seoul National University, Seoul 151-742, South Korea

E-mail: jklee@hep1.snu.ac.kr, solsen@hep1.snu.ac.kr

We are in the process of measuring the branching fractions of the decay $B^+ \rightarrow p\bar{p}K^+$ for the intermediate $c\bar{c}$ states $\psi(3770)$, $X(3872)$, and $Y(3915)$ decaying to $p\bar{p}$, using a 711 fb^{-1} data sample collected on the $\Upsilon(4S)$ resonance by the Belle detector at the KEKB asymmetric-energy e^+e^- collider. The analysis is performed as a blind analysis in which the $p\bar{p}$ mass region $3.7 \text{ GeV}/c^2$ to $4.0 \text{ GeV}/c^2$ is blinded. In this document, we report the preliminary results before unblinding the box and the measured branching fractions of $\eta_c \rightarrow p\bar{p}$, and $J/\psi \rightarrow p\bar{p}$, whose mass peaks are outside the blinded region.

XV International Conference on Hadron Spectroscopy-Hadron 2013

4-8 November 2013

Nara, Japan

^{*}Speaker.

[†]On behalf of the Belle Collaboration

1. Introduction

Although there have been many observations of charmoniumlike states in recent years, decay mechanism is still not clearly understood. We study the $B^+ \rightarrow (c\bar{c})K^+$ decays followed by the $c\bar{c}$ states, including $\psi(3770)$, $X(3872)$, and $Y(3915)$, decay to $p\bar{p}$. The searches are based on a blind analysis in which the $p\bar{p}$ mass region $3.7 \text{ GeV}/c^2$ to $4.0 \text{ GeV}/c^2$ is blinded. In this document, we report the preliminary results before unblinding the box and the measured branching fractions of $\eta_c \rightarrow p\bar{p}$, and $J/\psi \rightarrow p\bar{p}$, whose mass peaks are outside the blinded region.

2. Detector Description

The Belle detector is a large-solid-angle magnetic spectrometer that consists of a silicon vertex detector (SVD), a 50-layer cylindrical drift chamber (CDC), an array of aerogel threshold Cherenkov counters (ACC), a barrel-like arrangement of time-of-flight scintillation counters (TOF), and an electromagnetic calorimeter (ECL) comprised of CsI(Tl) crystals located inside a superconducting solenoid coil that provides a 1.5 T magnetic field. An iron flux-return located outside of the coil is instrumented to detect K_L mesons and to identify muons (KLM). The detector is described in detail elsewhere [1, 2].

3. Data and Event Selection

This study is based on a data sample with an integrated luminosity of 711 fb^{-1} , containing $772 \times 10^6 \text{ } B\bar{B}$ pairs, collected with the Belle detector at the KEKB asymmetric energy e^+e^- (3.5 on 8 GeV) collider.

All primary charged tracks are required to originate from within $\pm 1 \text{ cm}$ in the radial direction, and within $\pm 3 \text{ cm}$ along the beam direction of the interaction point (IP). Measurements of dE/dx in the CDC, light yields in the ACC and flight times in the TOF are combined to form particle identification (id) likelihoods $\mathcal{L}(h)$ ($h = \pi^+, K^+$ or p) for charged hadronic tracks. Hadron id assignments are based on the likelihood ratios

$$R(h|h') = \frac{\mathcal{L}(h)}{\mathcal{L}(h) + \mathcal{L}(h')}. \quad (3.1)$$

For each track, the track is assigned as a proton if $R(p|K) > 0.6$ and $R(p|\pi) > 0.6$, as a kaon if $R(K|\pi) > 0.6$, or as a pion if $R(\pi|K) > 0.6$.

The reconstructed B meson candidates are identified by the beam-energy-constrained mass $M_{bc} = \sqrt{E_{\text{beam}}^2 - p_B^2}$, and the energy difference $\Delta E = E_B - E_{\text{beam}}$, where E_{beam} is the beam energy, and p_B and E_B are the momentum and energy, respectively, of the reconstructed B meson in the rest frame of the $\Upsilon(4S)$. The signal region is defined as $5.27 \text{ GeV}/c^2 < M_{bc} < 5.29 \text{ GeV}/c^2$ and $|\Delta E| < 0.05 \text{ GeV}$.

The continuum events, $e^+e^- \rightarrow q\bar{q}$ where $q = u, d, s$, and c are the dominant background for charmless B decays since $e^+e^- \rightarrow q\bar{q}$ events have about a three-times larger cross section than $e^+e^- \rightarrow \Upsilon(4S) \rightarrow B\bar{B}$ events. To discriminate the "spherical" $B\bar{B}$ events from the "back-to-back" jet-like continuum $q\bar{q}$ events, two kinds of event shape variables are chosen: the KSF (Kakuno-Super-Fox-Wolfram) [3], the modified SF with 17 Fisher coefficients [4, 5, 6], and $\cos\theta_B$, the

cosine of the angle between the B flight direction and the beam direction in the $\Upsilon(4S)$ rest frame. For the signal sample, we generate MC sample corresponding to $B^+ \rightarrow p\bar{p}K^+$. The background sample is obtained from the continuum background MC. The calculated individual likelihood ratio for KSFW and $\cos\theta_B$ are combined to form a total likelihood ratio $\mathcal{L}\mathcal{R}_{total}$. The selection point is determined based on the figure of merit ($n_S/\sqrt{n_S+n_B}$) study, where n_S (n_B) is the expected numbers of signal (background) in the signal box. To estimate the expected signal yield, we assume $\mathcal{B}(B^+ \rightarrow p\bar{p}K^+) = 5.9 \times 10^{-6}$ (PDG). The number of background in the signal box is estimated from the continuum background MC. We require the total likelihood ratio to be $\mathcal{L}\mathcal{R}_{total} > 0.75$. Multiple B candidates per event are allowed; the fraction of events involved is found to be 7%.

4. Preliminary Results

The signal yield is determined from a two-dimensional unbinned likelihood fit to the $\Delta E - M_{bc}$ distributions. The signal PDF is composed of a single Gaussian for the M_{bc} and a double Gaussian for ΔE . The background PDF is composed of the ARGUS function for M_{bc} , and a second-order polynomial for ΔE . The parameters of the signal PDFs and the ARGUS function are fixed to the values determined by the $J/\psi \rightarrow p\bar{p}$ control samples with $3.0751 \text{ GeV}/c^2 < M_{p\bar{p}} < 3.1179 \text{ GeV}/c^2$ corresponding to a $\pm 3\sigma$ region around the J/ψ mass peak. The coefficients of the background PDF for ΔE are fit parameters. The M_{bc} distributions with $|\Delta E| < 0.05 \text{ GeV}$ and the ΔE distributions with $M_{bc} > 5.27 \text{ GeV}/c^2$ for all $M_{p\bar{p}}$ region are shown in Figure 1. We observe 2429 ± 59 reconstructed $B^+ \rightarrow p\bar{p}K^+$ events.

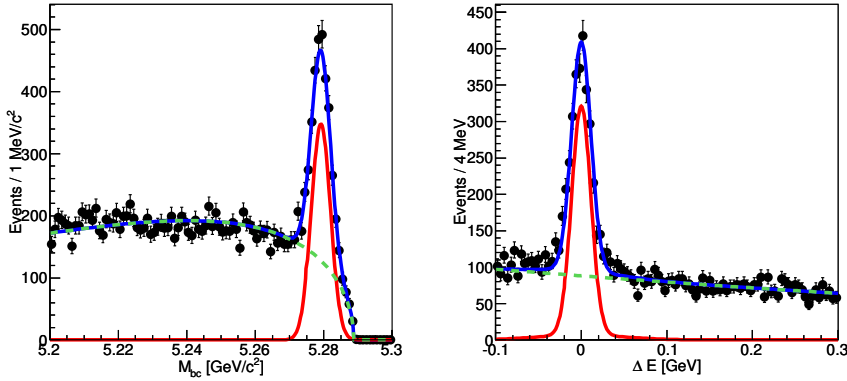


Figure 1: The M_{bc} with $|\Delta E| < 0.05 \text{ GeV}$ and ΔE with $M_{bc} > 5.27 \text{ GeV}/c^2$ distributions for $B^+ \rightarrow p\bar{p}K^+$ candidates. The red solid curve, the green dotted curve, and the blue solid curve overlaid on histogram represent the 2D fit projection of signal, background, and the combined result, respectively.

The fitted yields are corrected by the detection efficiencies determined from a MC sample generated uniformly in all $M_{p\bar{p}}$ region to calculate partial branching fraction for each $M_{p\bar{p}}$ bin. Figure 2 shows the fitted yield divided by bin size (left) and the differential branching fraction (right) for $B^+ \rightarrow p\bar{p}K^+$ as a function of $M_{p\bar{p}}$; these are compared with previous published results with 414 fb^{-1} data (blue) [7]. The sensitive $M_{p\bar{p}}$ region between $3.7 \text{ GeV}/c^2$ and $4.0 \text{ GeV}/c^2$ is blinded. The fitted yields, the efficiencies, and the branching fractions for each $M_{p\bar{p}}$ bin are listed in Table 1.

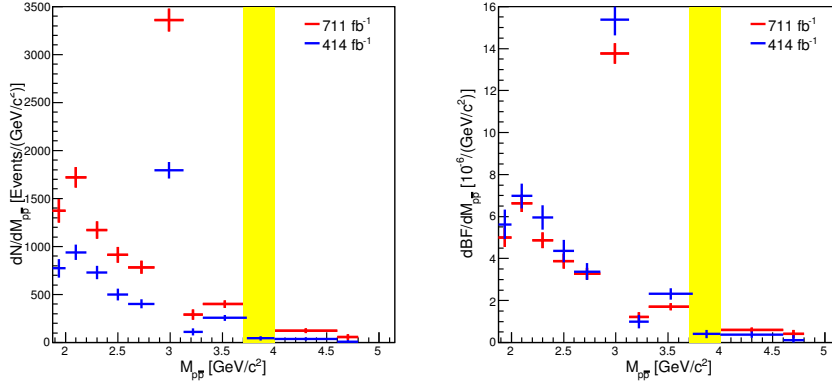


Figure 2: The fitted B yields divided by bin size (left) and the differential branching fractions (right) for $B^+ \rightarrow p\bar{p}K^+$ as a function of $M_{p\bar{p}}$ (red points with error bars). The results with 414 fb^{-1} data [7] are superimposed with blue markers.

$M_{p\bar{p}}$ (GeV/ c^2)	Yield	eff (%)	$\mathcal{B} (\times 10^{-6})$
1.876 - 2.0	170.0 ± 15.2	35.2 ± 0.2	0.63 ± 0.06
2.0 - 2.2	344.3 ± 21.6	33.0 ± 0.2	1.35 ± 0.08
2.2 - 2.4	234.5 ± 18.1	30.4 ± 0.2	1.00 ± 0.08
2.4 - 2.6	182.6 ± 16.4	29.3 ± 0.2	0.80 ± 0.07
2.6 - 2.85	195.9 ± 16.7	29.5 ± 0.2	0.86 ± 0.07
2.85 - 3.128	934.1 ± 32.8	29.6 ± 0.1	4.09 ± 0.14
3.128 - 3.315	54.2 ± 9.8	28.6 ± 0.2	0.25 ± 0.04
3.315 - 3.735	168.3 ± 16.6	28.1 ± 0.1	0.78 ± 0.08
3.735 - 4.0	—	—	—
4.0 - 4.6	74.3 ± 14.2	26.6 ± 0.1	0.36 ± 0.07
4.6 - 4.8	11.5 ± 5.7	18.2 ± 0.2	0.08 ± 0.04

Table 1: The fitted B yields, detection efficiencies, and branching fractions in different $M_{p\bar{p}}$ regions. The errors include only statistical uncertainties.

Figure 3 shows the differential branching fraction as a function of $M_{p\bar{p}}$ in the $\eta_c - J/\psi$ mass region. There are clear η_c , and $J/\psi \rightarrow p\bar{p}$ peaks. To calculate the branching fractions $\mathcal{B}(\eta_c \rightarrow p\bar{p})$ and $\mathcal{B}(J/\psi \rightarrow p\bar{p})$, a binned χ^2 fit to 1 dimensional $M_{p\bar{p}}$ histogram is performed. The Voigtian function with the full width Γ fixed to 0.0297 GeV (PDG) for the η_c peak, a single Gaussian function for the J/ψ peak, and a linear function for the background are used. Except the Γ of the Voigtian function, all parameters are allowed to float. The combined fitting function is shown as the blue solid curve in Figure 3. The measured masses are $2975.9 \pm 2.4 \text{ MeV}/c^2$ for the η_c , and $3096 \pm 0.9 \text{ MeV}/c^2$ for the J/ψ . The product branching fractions $\mathcal{B}(B^+ \rightarrow \eta_c K^+) \times \mathcal{B}(\eta_c \rightarrow p\bar{p})$ and $\mathcal{B}(B^+ \rightarrow J/\psi K^+) \times \mathcal{B}(J/\psi \rightarrow p\bar{p})$ are measured to be $(1.38 \pm 0.11) \times 10^{-6}$ and $(2.05 \pm 0.11) \times 10^{-6}$, respectively. The results are summarized in Table 2.

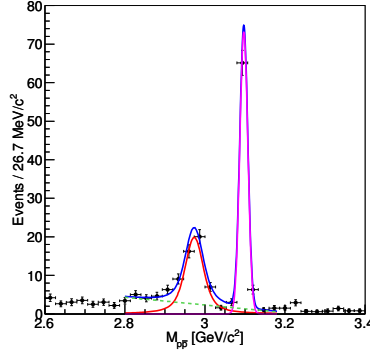


Figure 3: Differential branching fraction for $B^+ \rightarrow p\bar{p}K^+$ as a function of $M_{p\bar{p}}$ in the $\eta_c - J/\psi$ mass region. The red solid curve, purple solid curve, green dotted curve, and blue solid curve represent the fitted η_c signal, fitted J/ψ signal, fitted background, and the combined fit results, respectively.

Modes	Mass (MeV/ c^2)	Yield	Product branching fraction
$B^+ \rightarrow \eta_c K^+, \eta_c \rightarrow p\bar{p}$	2975.9 ± 2.4	306.64 ± 20.90	$(1.38 \pm 0.11) \times 10^{-6}$
$B^+ \rightarrow J/\psi K^+, J/\psi \rightarrow p\bar{p}$	3096.8 ± 0.9	468.12 ± 22.72	$(2.05 \pm 0.11) \times 10^{-6}$

Table 2: The measured $\eta_c, J/\psi$ masses and the fitted signal yields and branching fractions for $\eta_c, J/\psi \rightarrow p\bar{p}$. The errors include only statistical uncertainties.

5. Summary

In summary, using $772 \times 10^6 B\bar{B}$ events, we search for the decays $(c\bar{c}) \rightarrow p\bar{p}$ from $B^+ \rightarrow p\bar{p}K^+$ decays. The differential branching fraction versus $M_{p\bar{p}}$ distribution was obtained with the sensitive signal region blinded. The preliminary results are consistent with the previous published results with $414 fb^{-1}$ [7]. We also measure the branching fractions of $\eta_c \rightarrow p\bar{p}$, and $J/\psi \rightarrow p\bar{p}$, which are consistent with the PDG values.

References

- [1] A. Abashian *et al.* (Belle Collaboration), *The Belle detector*, *Nucl. Instr. Meth. A* **479**, 117 (2002).
- [2] J. Brodzicka *et al.* (Belle Collaboration), *Physics achievements from the Belle experiment*, *Prog. Theor. Exp. Phys.* **2012**, 04D001 (2012) [arXiv:1212.5342].
- [3] S.H. Lee *et al.* (Belle Collaboration), *Evidence for $B^0 \rightarrow \pi^0\pi^0$* , *Phys. Rev. Lett.* **91**, 261801 (2003).
- [4] G. Fox and S. Wolfram, *Observables for the Analysis of Event Shape in e^+e^- Annihilation and Other Processes*, *Phys. Rev. Lett.* **41**, 1581 (1978).
- [5] R.A. Fisher, *The Use of Multiple Measurements in Taxonomic Problems*, *Annals of Eugenics* **7**, 179 (1936).
- [6] K. Abe *et al.* (Belle Collaboration), *Measurement of the Branching Fraction for $B \rightarrow \eta' K$ and Search for $B \rightarrow \eta' \pi^+$* , *Phys. Lett. B* **517** (2001).
- [7] J.-T. Wei *et al.* (Belle Collaboration), *Study of the decay mechanism for $B^+ \rightarrow p\bar{p}K^+$ and $B^+ \rightarrow p\bar{p}\pi^+$* , *Phys. Lett. B* **659** (2008).